2016 14th International Conference on Control, Automation, Robotics & Vision
Phuket, Thailand, 13-15th November 2016 (ICARCV 2016)

Model Predictive Motion Control of Autonomous Forklift Vehicles with Dynamics Balance Constraint

Alireza Mohammadi*, Iven Mareels* and Denny Oetomo*
*Melbourne School of Engineering, The University of Melbourne, Parkville VIC 3010, Australia
Email: {alirezam,i.mareels, doetomo}@unimelb.edu.au

***Abstract*—In this paper, a model predictive control is developed for motion planning and control of nonholonomic autonomous forklifts. The proposed model predictive motion control (MPMC) determines the control inputs for tracking a desired path through minimising path-following error, subject to nonholonomic and dynamic balance constraints of the forklift. MPMC also automatically adjusts the tracking velocity and acceleration to traverse the path as fast as possible without violating constraints while minimising the tracking error. In order to facilitate the real-time implementation of MPMC for industrial applications, a successive online linearisation of the nonlinear discrete-time kinematic model of the forklift is employed along with linear time-varying approximation of the tracking errors. The effectiveness of the proposed method has been demonstrated through simulations.**

I. INTRODUCTION

Forklifts are the most common goods handling vehicles extensively used in different types of industries. In recent years, there has been a growing interest in automating the forklift vehicles in order to minimise human mistakes and improve the operational safety [1]–[4]. This paper focuses on motion control of autonomous forklifts. Motion controllers aim at controlling the vehicle to track a predetermined geometric path generated by path planning algorithms.

In industrial autonomous forklifts, it is required to track a geometrically planned path in the shortest time with maximum path tracking accuracy while subject to dynamic balance constraints to prevent it from toppling in a constrained space such as warehouse. Toppling is a concern for forklift vehicles where high accelerations, velocities and sharp turns are concerned but added to this is the ability to move the forks and handle a payload.

In [4]–[7], forklifts are considered as mobile robots while motion planning of mobile robots has focused on low speeds which ignores the momentum of the robot. In some other literature [8], [9], forklifts are treated as mobile manipulators which takes into account the dynamic stability in motion planning and control algorithms. However, these algorithms require dynamic parameters such as torques, forces and frictions to be estimated for modelling, which in general is difficult, particularly in industrial applications.

Moreover, most of the existing motion controllers for mobile manipulators are based on the trajectory tracking algorithms whereby a path generation algorithm at a higher level convert the desired path to a time-dependent reference trajectory and then at a lower level controller is used to reduce the trajectory tracking error. However, an alternative approach is to minimise path tracking error, defined as the normal distance between the current position of the forklift and the desired path [10]. Therefore, it is not necessary to track the time parameterised reference trajectory accurately, as long as the system follows the desired path.

Path tracking algorithms typically results in a smoother convergence to a path for path-following controllers in comparison to trajectory tracking ones [11]. Moreover, it provides an extra degree of freedom in selecting the tracking speed. This is in particular is of interest in the cases that the path is required to be traversed at high speed to maximise productivity, specially in industrial applications [12]. However, due to vehicle balance constraints and system dynamics, this may lead to reduced accuracy which results in a compromise between tracking speed and accuracy. Therefore, time optimal planning of the reference trajectory should be considered while respecting system dynamic balance constraints.

The authors [13] have recently proposed a dynamic balance metrics based on zero moment point and barycentric coordinate system that calculates constraints on forklift velocity and accelerations. The advantage of this method is that it only requires inertia and centre of gravity (CoG) of the forklift. In this paper ,the proposed dynamic balance metrics is incorporated in trajectory planner without considering path-following and motion control of the forklift.

The model predictive control (MPC) is one of the promising controllers that can handle the constrains and address time-optimal requirements of the system. In [14], a model predictive based path-following control (MPFC) is used to combine nonlinear MPC approaches with time-optimal path tracking control. The MPFC essentially plans and follows the path within the same control loop and removes the need for a higher level control to adjust the path speed for trajectory generation. Nevertheless, the MPFC in [14] requires solving nonlinear optimisation problem which is difficult for real-time applications. An extension of the MPFC framework for real-time implementation is proposed in [15] denoted as model predictive contouring control (MPCC). This controller also takes into account the trade-off between productivity and accuracy in the cost function in contrast to MPFC which tries to drive the path-following error to zero. However, MPCC is only considered for linear systems and formulated for biaxial contouring control applications.

The objective of this paper is to propose model predictive motion control (MPMC) as an extension of [14] and [15] for

978-1-5090-3549-6/16/$31.00

motion planning and control of nonholonomic autonomous forklifts. The MPMC provides a comprehensive framework that integrates the constraint handling capabilities of MPC with time-optimal motion planning and control of forklifts, while also allowing real-time implementation of the control scheme.

The compromise between speed and accuracy of the autonomous forklift is also addressed by the choice of weights in the cost function similar to [15]. This allows the autonomous forklift to deviate from the desired path in order to traverse the path at higher speed. Moreover, in contrast to continuous feedback controller that requires taking into account the nonholonomic constraints of the forklift in path generation stage, the MPMC is able to handle the nonholonomic constraints of the forklift in one optimisation loop. The computational burden due to the nonlinear MPC structure of path-following control is also reduced by successive online linearisation of the plant model and desired path function about the current operating point at each time step.

II. Kinematic Model of Nonholonomic Autonomous Forklift

Consider the kinematic model of a nonholonomic autonomous forklift with rear driving-steering wheel in the inertial frame $x-y$ as (Fig. 1):

$$\begin{bmatrix} \dot{x} \\ \dot{y} \\ \dot{\theta} \\ \dot{\alpha} \end{bmatrix} = \begin{bmatrix} \cos\theta\cos\alpha & 0 \\ \sin\theta\cos\alpha & 0 \\ 1/R & 0 \\ 0 & 1 \end{bmatrix} \begin{bmatrix} v \\ \omega \end{bmatrix} \tag{1}$$

where x and y are the forklift positions and θ is the forklift orientation in the Cartesian inertial frame, α is the steering angle, v is the linear velocity of the driving wheel, ω is the the angular velocity of the steering wheel and R is the radius of the forklift instantaneous centre of rotation. R is also the radius of curvature, $R = l/\sin\alpha$ where l is the length of forklift. The distance between the two passive wheels at points B and C is defined as forklift track, d.

The body frame $x_b - y_b$ is centred at point O and the kinematic model in this frame is:

$$\begin{bmatrix} \dot{x_b} \\ \dot{y_b} \\ \dot{\theta} \\ \dot{\alpha} \end{bmatrix} = \begin{bmatrix} 1 & 0 \\ 0 & 0 \\ 1/R & 0 \\ 0 & 1 \end{bmatrix} \begin{bmatrix} v \\ \omega \end{bmatrix} \tag{2}$$

This frame will be used used in the dynamic balance calculations as explained in the following section.

As mentioned in the Introduction, in order to reduce the computational burden, a linear time-varying model of the forklift is used in MPMC. Consider the following linear time-varying discrete-time kinematic model of a nonholonomic forklift:

$$\xi_{k+1} = A_k\xi_k + B_k u_k, \tag{3}$$

where $\xi_k = [x_k \ y_k \ \theta_k \ \alpha_k]^T$, $u_k = [v_k \ w_k]^T$ and A_k, B_k are:

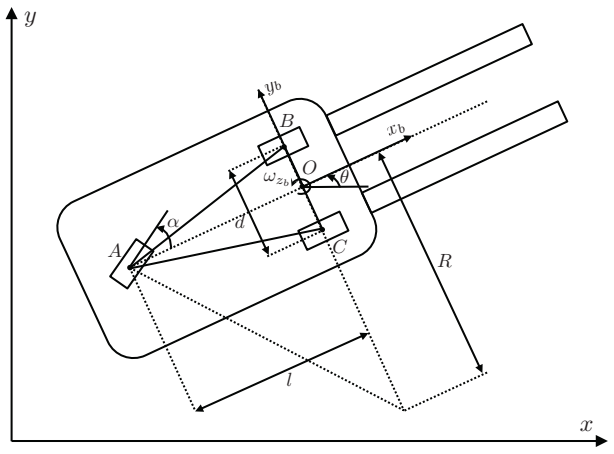

Fig. 1. Schematic of Non-collocated rotor and stator

$$A_k = \begin{bmatrix} 1 & 0 & -T_s\sin(\theta_k)\cos(\alpha_k)v_k & -T_s\cos(\theta_k)\sin(\alpha_k)v_k \\ 0 & 1 & T_s\cos(\theta_k)\cos(\alpha_k)v_k & -T_s\sin(\theta_k)\sin(\alpha_k)v_k \\ 0 & 0 & 1 & T_s\cos(\alpha_k)/l v_k \\ 0 & 0 & 0 & 1 \end{bmatrix}$$

$$B_k = \begin{bmatrix} T_s\cos(\theta_k)\cos(\alpha_k) & 0 \\ T_s\sin(\theta_k)\sin(\alpha_k) & 0 \\ T_s\sin(\alpha_k)/l & 0 \\ 0 & T_s \end{bmatrix},$$

where k states the current time step and T_s is the sample time. The forklift system is subject to input and state constraints due to the limits for linear and angular velocity and accelerations of the driving wheel in addition to dynamic balance constraints as explained in the following section.

III. Dynamic Balance Constraints

The dynamic balance is considered in the form of the zero moment point (ZMP) [13] . The ZMP describes a point on a flat surface that no moments acting on the system. If the ZMP lies within the support polygon (SP), the convex polygon ABC in Fig. 1, then the system is dynamically balanced. The d'Alembert formulation of the ZMP for the forklift shown in Fig. 1, assuming symmetric structure around y axis, can be represented as:

$$x_{ZMP} = x_{CoG} - z_{CoG}(\frac{a_{x_b}}{g}) + \frac{I_{Gyz}}{mg}\omega_z{}^2 \tag{4}$$

$$y_{ZMP} = y_{CoG} - z_{CoG}(\frac{a_{y_b}}{g}) + \frac{I_{Gyz}}{mg}\alpha_z \tag{5}$$

$$z_{ZMP} = 0 \tag{6}$$

where $(x_{CoG}, y_{CoG}, z_{CoG})$ is the position of centre of gravity (CoG) in body frame $x_b - y_b - z_b$, I_{Gyz} is the second moment of inertia around $y_b - z_b$, a_{x_b} and a_{y_b} accelerations in x_b and y_b direction, m is the overall mass of the forklift and load and $\omega_{z_b} = \dot{\theta}$ and $\alpha_{z_b} = \ddot{\theta}$ are the angular velocity and acceleration of the forklift around z_b axis at point O.

It should be noted that this formulation of the ZMP assumes planar motion. This assumption may be used if we consider many forklifts experience only planar surfaces such as in a warehouse environment, or freight distribution centre.

Considering the ZMP inside the SP of the forklift, then the constraints on ZMP will result in the following inequalities:

$$x_{ZMP} < 0 \tag{7}$$
$$y_{ZMP} < -\frac{d}{2l}x_{ZMP} - \frac{d}{2} \tag{8}$$
$$y_{ZMP} < -\frac{d}{2l}x_{ZMP} + \frac{d}{2} \tag{9}$$
$$\tag{10}$$

Substituting x_{ZMP} and y_{ZMP} in these equations leads to the following constraints on forklift velocities and accelerations:

$$M \begin{bmatrix} a_{x_b} \\ a_{y_b} \\ \omega_{z_b}^2 \\ \alpha_{z_b} \end{bmatrix} < N \tag{11}$$

where

$$M = \begin{bmatrix} -\frac{z_{CoG}}{g} & 0 & \frac{I_{Gyz}}{mg} & 0 \\ \frac{z_{CoG}}{g} & -\frac{2l}{d}\frac{z_{CoG}}{g} & -\frac{I_{Gyz}}{mg} & \frac{2l}{d}\frac{I_{Gyz}}{mg} \\ \frac{z_{CoG}}{g} & \frac{2l}{d}\frac{z_{CoG}}{g} & -\frac{I_{Gyz}}{mg} & -\frac{2l}{d}\frac{I_{Gyz}}{mg} \end{bmatrix}$$

$$N = \begin{bmatrix} -x_{CoG} \\ x_{CoG} - \frac{2l}{d}y_{CoG} + l \\ x_{CoG} + \frac{2l}{d}y_{CoG} + l \end{bmatrix}$$

The above inequality shows that the calculation of the constraints on forklift velocities and accelerations only requires position of CoG, inertial, size and mass of the forklift. Additionally, considering the kinematic model of the forklift in the body frame, we obtain: $a_{x_b} = \dot{v}$, $x_{y_b} = 0$, $\omega_{z_b} = \dot{\theta}$ and $\alpha_{z_b} = \ddot{\theta}$. As a result, dynamic balance requirement implies constraints on the inputs and states of the the forklift kinematic model.

IV. Path-following Formulation

The purpose of the path-following algorithm is to produce control signal (v, ω) such that the forklift follows a given geometric path with maximum feasible speed without violating the forklift dynamic balance constraints.

Consider the desired path as $(x^d(\psi), y^d(\psi))$ which is parameterised by path length ψ. Using spline curves for approximation of the path length [16], for each path parameter ψ, $x^d(\psi)$ and $y^d(\psi)$ can be calculated. Assuming the desired velocity of path following, v^d, and path parameter, ψ as the distance travelled along the path, the following dynamics is amended to the kinematic model (3):

$$\psi_{k+1} = \psi_k + v_k^d, \qquad |v_k^d| < v_{max}^d \tag{12}$$

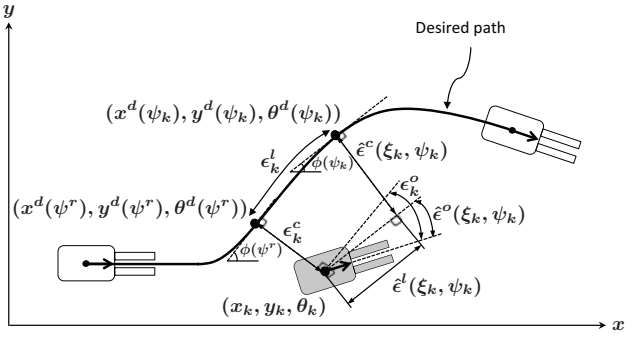

Fig. 2. Path-following errors of a nonholonomic autonomous forklift

where v_k^d is an extra input to be determined by the controller at time step k. It should be noted that based on the above equation, forklift can traverse the path in reverse direction.

As shown in Fig. 2, the path-following error is defined similar to [10] as the normal deviation from the desired path, ε^c. However, the calculation of the reference path parameter ψ^r and therefore the error ε^c is not practical in real-time implementations. As a result, ψ_k which is defined in (12) is used as an approximation of ψ_r. With this approximation, the path-following errors are obtained as:

$$\hat{\varepsilon}^c = (x_k - x^d(\psi_k))\sin\phi(\psi_k) - (y_k - y^d(\psi_k))\cos\phi(\psi_k), \tag{13}$$
$$\hat{\varepsilon}^l = (x^d(\psi_k) - x_k)\cos\phi(\psi_k) - (y_k - y^d(\psi_k))\sin\phi(\psi_k), \tag{14}$$
$$\hat{\varepsilon}^o = \phi(\psi_k) - \theta, \tag{15}$$

and

$$\phi(\psi_k) = \arctan\left(\frac{y^d(\psi_k) - y^d(\psi_{k-1})}{x^d(\psi_k) - x^d(\psi_{k-1})}\right), \tag{16}$$

where $\hat{\varepsilon}^c$, $\hat{\varepsilon}^l$ and $\hat{\varepsilon}^o$ are approximations of the cross-track, longitudinal and orientational errors.

After introducing the path-following errors, the cost function for model predictive motion control (MPMC) formulation at time step k is considered as:

$$J_k = \sum_{i=1}^{N} \left(\hat{\varepsilon}_{k+i,k}^T Q_\varepsilon \hat{\varepsilon}_{k+i,k} - q_\psi \psi_{k+i,k} + \Delta\bar{u}_{k+i-1,k}^T R_u \Delta\bar{u}_{k+i-1,k}\right), \tag{17}$$

where

$$\hat{\varepsilon}_{k+i,k} = \begin{bmatrix} \hat{\varepsilon}^c(\xi_{k+i,k}, \psi_{k+i,k}) \\ \hat{\varepsilon}^l(\xi_{k+i,k}, \psi_{k+i,k}) \\ \hat{\varepsilon}^o(\xi_{k+i,k}, \psi_{k+i,k}) \end{bmatrix}, \Delta\bar{u}_{k+i-1,k} = \begin{bmatrix} \Delta u_{k+i-1,k} \\ \Delta v_{k+i-1,k}^d \end{bmatrix}$$

$$\Delta u_{k+i-1,k} = u_{k+i-1,k} - u_{k+i-2,k}$$
$$\Delta v_{k+i-1,k} = v_{k+i-1,k} - v_{k+i-2,k}$$
$$Q_\varepsilon = \begin{bmatrix} q_c & 0 & 0 \\ 0 & q_l & 0 \\ 0 & 0 & q_o \end{bmatrix}, \quad q_c, q_l, q_o, q_\psi > 0, \quad R_u \in R_{>0}^3$$

where N is the prediction horizon, the subscript $k+i,k$ denotes the prediction at time $k+i$ predicted at time k, Q_ε, q_ψ and R are the weighs coefficients reflecting the relative importance

of path-following error, path-following speed and changes in the control inputs.

Since the desired path $(x^d(\psi_k), y^d(\psi_k))$ is nonlinear function of ψ in the path-following errors, the cost function (17) leads to nonlinear optimisation problem. In order to reduce the computational effort for real-time implementation using linearisation and at the same time keep the linearisation error small, the nonlinear path function is linearised around operating point of the system. This leads to linear time-varying approximation of the path-following errors.

Then, implementation of the LTV MPMC for path-following of a nonholonomic autonomous forklift can be obtained through solving the following optimisation problem using quadratic programming (QP) approach:

$$\begin{aligned}
&\text{Minimize} && J_k \\
&\text{Subject to} && \xi_{k+1} = A_k\xi_k + B_k u_k, \\
&&& \psi_{k+1} = \psi_k + v_k^d, \\
&&& \psi_{k,k} = \psi_k, \\
&&& M\ [a_{x_b}\ a_{y_b}\ \omega_{z_b}^2\ \alpha_{z_b}]^T < N, \\
&&& |v_k^d| < v_{max}^d \\
&&& 0 \le \theta_k < \pi/2 \\
&&& u_{min} \le u \le u_{max}
\end{aligned} \tag{18}$$

The implementation procedure is summarised in the following algorithm:

Algorithm 1 Implementation of LTV MPMC algorithm

1: Initialise the desired speed $v^d(0)$ and forklift states $\xi(0)$
2: Calculate path parameter ψ using desired speed $v^d(0)$
3: Linearise desired path (x^d, y^d) around ψ
4: Compute dynamic balance constraints using (11)
5: Solve optimisation problem (18)
6: Send the first element of u
7: Calculate path parameter ψ using current v^d
8: Go to **Step 3**

V. Main Features of MPMC for Industrial Applications

In this section, the main features and capabilities of the MPMC in comparison to the existing approaches are highlighted.

First of all, in contrast to the trajectory tracking algorithms which requires the path speed to be determined in advance in a separate high level path generation procedure, MPMC automatically adjusts the path speed v_k^d at each step of the optimisation.

Secondly, the trade-off between path-following accuracy and speed is reflected in the optimisation problem through adjusting the weighting matrices Q_ε and q_ψ, respectively. Therefore, in the cases that it is desired to traverse the path faster while allowing the forklift to deviate from the desired path, the higher q_ψ is used in the formulation (17). It should be noted that productivity of the forklift operation depends on both accuracy and speed. For instance, if the desired path is the shortest path between the start and end point of the forklift operation, large deviation from the path to move faster will result in travelling longer path that may lead to lower productivity. Therefore, an appropriate tuning of the weighting matrices is required depending on the definition of the productivity for a specific forklift.

Thirdly, the dynamic balance constraints of the forklift (11) is included in the optimisation problem which ensures the stability of the forklift at all conditions. Due to the use of LTV approach for MPMC, the dynamic balance constraints can be time-varying as well. For instance, if CoG of the forklift changing during the path-following procedure, due to change of the load position, this variation can be updated in the next step of the optimisation problem.

Finally, the nonholonomic constraints of the forklift are included in the optimisation problem through including the kinematic of the forklift as a constraint in the MPMC formulation (18). In most of the existing path tracking algorithms, the nonholonomic constraints should be explicitly taken into account in generation for the desired path. For example, different approaches such as Simple Continuous Curvature (SCC) [17] and Double Continuous Curvature (DCC) [18] are used to produce continuous curvature path for tracking of the forklift. As a result, simple optimal algorithms such as Dubins' path which does not satisfy the nonholonomic constraints, can be used as a desired path for MPMC.

VI. Simulation Results

In this section, the proposed MPMC is demonstrated using a three wheeled miniature forklift model for tracking a given geometric path. This miniature forklift will be used in the future to experimentally verify the approach before use on real forklifts. This miniature forklift resembles the Hyster R1.4 Reach Truck. The dimensions of the miniature forklift are summarised in Table I.

TABLE I
Miniature model forklift parameters

Parameter		Value	
Forklift length	l	0.5	m
Forklift track	d	0.6	m
Total mass of forklift and load		13.6	kg
CoG	$[x_{CoG}, y_{CoG}, z_{CoG}]$	$[-0.2, 0, 0.8]^T$	m
Moment of inertia	I_{Gyz}	0.17	$kg.m^2$

The desired path includes two segments, an arc and a straight line. It should be noted that the connections between these segments do not satisfy continuous curvature condition required with most of the path tracking controllers for nonholonomic vehicles.

The model predictive motion control was simulated for the forklift model to track a geometric path. The simulations are performed for different values of the path speed weighting, q_ψ, while keeping the other weighting constant with $N = 10$,

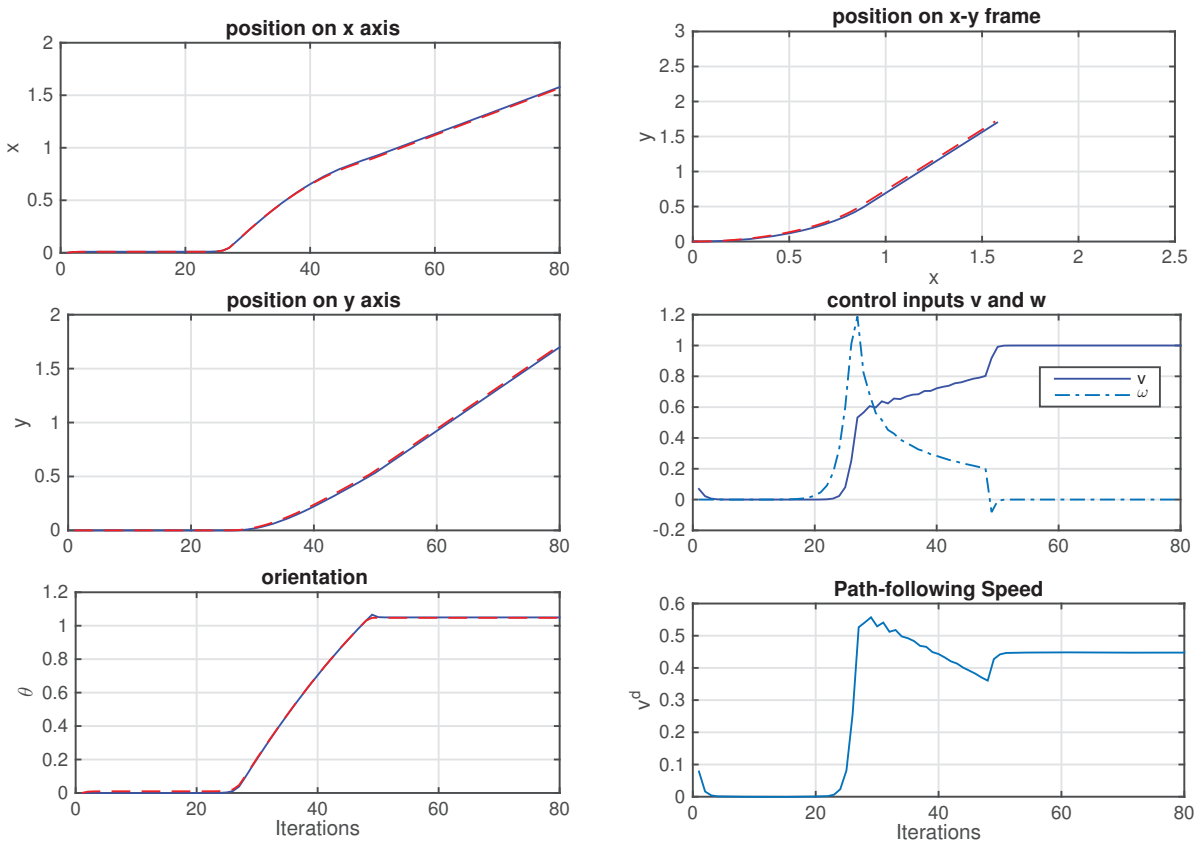

Fig. 3. Path-following results with path speed weighting q_ψ=2 and $z_{CoG} = 0.8$; red-dashed-line shows the desired path and corresponding states.

$Q_\varepsilon = 100 \times I$, and $R_u = 0.2 \times I$. The constraints on driving and steering speeds are $-1 \leq v \leq 1$ and $-1 \leq \omega \leq 1$, respectively. The initial conditions are $\xi(0) = [0;0;0;0]$ and $v^d(0) = 0$.

The path-following performance of the proposed MPMC with path speed weightings $q_\psi = 2$ is shown in Fig. 3. The simulated model forklift follows the desired path while respecting input and dynamic balance constraints. It traverses the path with lower speed while turning and then moves with maximum speed, $v = 1$, on the straight line segment.

The path-following results for $q_\psi = 10$ is shown in Fig. 4. The results show that for $q_\psi = 10$, the forklift traverse the path faster compared to $q_\psi = 2$ in Fig. 3, but the deviation from desired path is larger. This demonstrates the trade-off between path-following accuracy and speed as explained in Section V.

In order to evaluate the performance of MPMC when the dynamic balance constraints are varying, the location of CoG in z-axis is changed from $z_{CoG} = 0.8$ to $z_{CoG} = 1$. The results are shown in Fig. 5. It can be observed the path-following speed is lower while the forklift is turning and then tracks the path with maximum speed.

VII. Conclusions and Future Works

In this paper, a model predictive based motion control algorithm is developed for nonholonomic autonomous forklifts. The proposed algorithm integrates time-optimality with nonholonomic and dynamic balance constraint of the forklift while also allowing real-time implementation for industrial applications.

The simulation results demonstrated the effectiveness of the MPMC for motion control of autonomous forklifts. The implementation of the MPMC on a miniature forklift will be performed as the future work.

References

[1] T. A. Tamba, B. Hong, and K.-S. Hong, "A path following control of an unmanned autonomous forklift," *International Journal of Control, Automation and Systems*, vol. 7, no. 1, pp. 113–122, 2009.

[2] S. Teller, M. R. Walter, M. Antone, A. Correa, R. Davis, L. Fletcher, E. Frazzoli, J. Glass, J. P. How, A. S. Huang, *et al.*, "A voice-commandable robotic forklift working alongside humans in minimally-prepared outdoor environments," in *IEEE International Conference on Robotics and Automation (ICRA)*, pp. 526–533, 2010.

[3] M. Seelinger and J.-D. Yoder, "Automatic visual guidance of a forklift engaging a pallet," *Robotics and Autonomous Systems*, vol. 54, no. 12, pp. 1026–1038, 2006.

[4] D. Lecking, O. Wulf, and B. Wagner, "Variable pallet pick-up for automatic guided vehicles in industrial environments," in *IEEE Conference on Emerging Technologies and Factory Automation (ETFA)*, pp. 1169–1174, 2006.

[5] A. Widyotriatmo, A. K. Pamosoaji, and K.-S. Hong, "Robust configuration control of a mobile robot with uncertainties," in *Control Conference (ASCC), 2011 8th Asian*, pp. 1036–1041, IEEE, 2011.

[6] D. Herrero, J. Villagra, and H. Martinez, "Self-configuration of waypoints for docking maneuvers of flexible automated guided vehicles,"

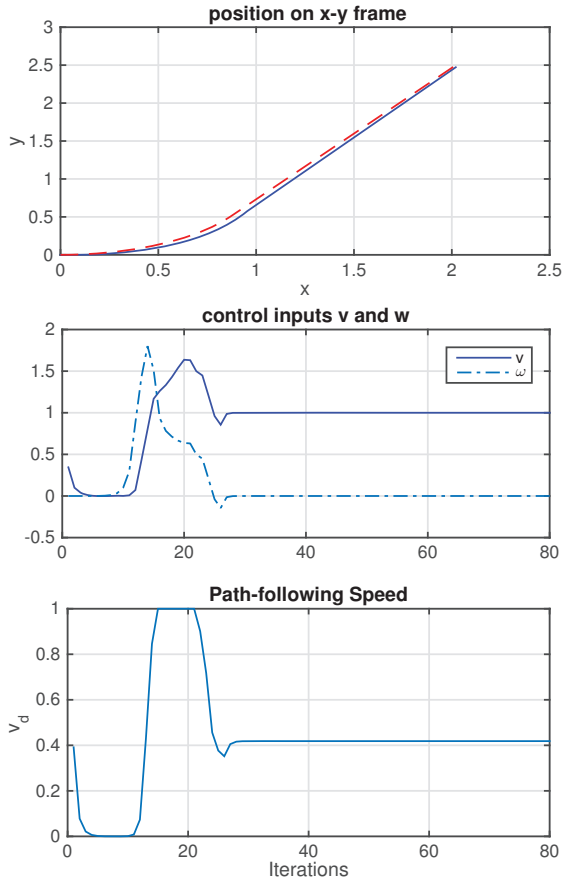

Fig. 4. Path-following results with path speed weighting q_ψ=10 and z_{CoG} = 0.8; red-dashed-line shows the desired path.

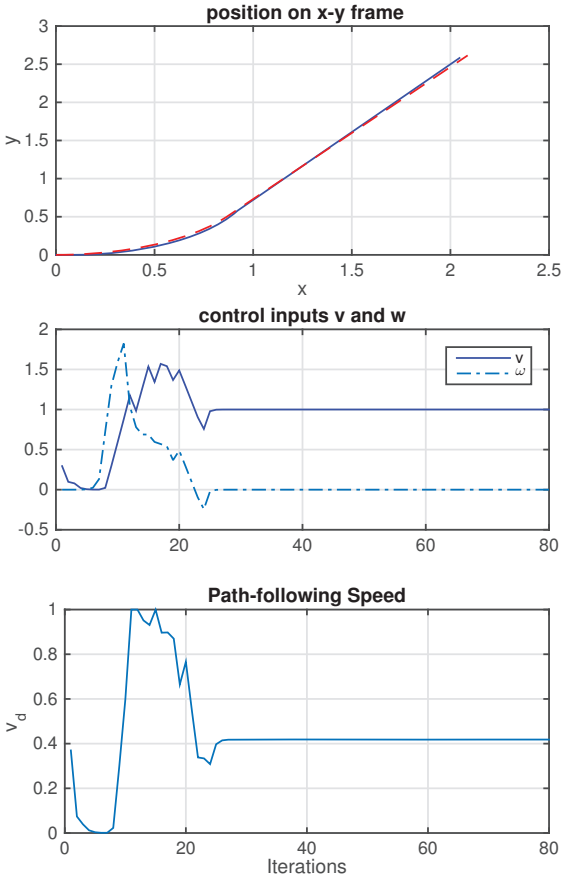

Fig. 5. Path-following results with path speed weighting q_ψ=10 and $z_{CoG} = 1$; red-dashed-line shows the desired path.

Automation Science and Engineering, IEEE Transactions on, vol. 10, no. 2, pp. 470–475, 2013.

[7] A. Widyotriatmo and K.-S. Hong, "Navigation function-based control of multiple wheeled vehicles," *Industrial Electronics, IEEE Transactions on*, vol. 58, no. 5, pp. 1896–1906, 2011.

[8] Y. Jia, N. Xi, Y. Cheng, and S. Liang, "Coordinated motion control of a nonholonomic mobile manipulator for accurate motion tracking," in *Intelligent Robots and Systems (IROS 2014), 2014 IEEE/RSJ International Conference on*, pp. 1635–1640, IEEE, 2014.

[9] T. Sugar and V. Kumar, "Decentralized control of cooperating mobile manipulators," in *Robotics and Automation, 1998. Proceedings. 1998 IEEE International Conference on*, vol. 4, pp. 2916–2921, IEEE, 1998.

[10] D. Lam, C. Manzie, and M. Good, "Model predictive contouring control," in *IEEE Conference on Decision and Control (CDC)*, pp. 6137–6142, 2010.

[11] K. Kanjanawanishkul, M. Hofmeister, and A. Zell, "Smooth reference tracking of a mobile robot using nonlinear model predictive control.," in *ECMR*, pp. 161–166, 2009.

[12] D. Lam, C. Manzie, and M. Good, "Application of model predictive contouring control to an xy table," in *Proc. of 18th IFAC World Congress, Milano, Italy*, pp. 10325–10330, 2011.

[13] L. Vongchanh, A. Mohammadi, A. Kealy, and D. Oetomo, "Dynamically balanced trajectory generation for non-holonomic forklift vehicles," *Australasian Conference on Robotics and Automation*, 2015.

[14] T. Faulwasser and R. Findeisen, "Nonlinear model predictive path-following control," in *Nonlinear Model Predictive Control*, pp. 335–343, Springer, 2009.

[15] D. Lam, C. Manzie, and M. Good, "Model predictive contouring control for biaxial systems," *IEEE Transactions on Control Systems Technology*, vol. 21, no. 2, pp. 552–559, 2013.

[16] H. Wang, J. Kearney, and K. Atkinson, "Arc-length parameterized spline curves for real-time simulation," in *5th international conference on Curves and Surfaces*, 2002.

[17] A. Scheuer and T. Fraichard, "Continuous-curvature path planning for car-like vehicles," in *IEEE/RSJ International Conference on Intelligent Robots and Systems (IROS)*, vol. 2, pp. 997–1003, 1997.

[18] V. Girbes, L. Armesto, and J. Tornero, "Path following hybrid control for vehicle stability applied to industrial forklifts," *Robotics and Autonomous Systems*, vol. 62, no. 6, pp. 910–922, 2014.